RESEARCH ARTICLE

INTERNATIONAL RESEARCH JOURNAL OF MULTIDISCIPLINARY TECHNOVATION

Asian Research Association

DOI: 10.54392/irjmt2621

Green Synthesized of Co_3O_4 Nanoparticles and Their Structural, Optical, Elastic, Morphological and Colloidal Stability

K. Leninbarathi [a,*], G. Bharath [b], S. Sathiyaraj [b], E. Ranjith Kumar [c], Ch. Srinivas [d], Vinayakprasanna N. Hegde [e], R.T. Karunakaran [a]

[a] Department of Physics, Government Arts College, Udumalpet-642154, Tamil Nadu, India

[b] Department of Chemistry, Sri Ramakrishna Mission Vidyalaya College of Arts and Science, Coimbatore-641020, Tamil Nadu, India.

[c] Department of Physics, KPR Institute of Engineering and Technology, Coimbatore-641407, Tamil Nadu, India

[d] JNTU-Kakinada Research Centre, Nanomaterials and Nanomagnetism Research Laboratory, Department of Physics, Sasi Institute of Technology & Engineering, Tadepalligudem-534101, Andhra Pradesh, India.

[e] Department of Physics, Vidyavardhaka College of Engineering, Mysuru-570002, Karnataka, India.

* Corresponding Author Email: physicsleninbarathik@gmail.com

DOI: https://doi.org/10.54392/irjmt2621

Received: 22-08-2025; Revised: 24-01-2026; Accepted: 07-02-2026; Published: 24-02-2026

Abstract: The current investigation successfully synthesised Co_3O_4 nanoparticles through a combustion method that employs a sustainable and economical approach, utilising the leaf, stem, and root extracts of the *Eichhornia crassipes* plant along with urea. The phytochemicals found in the plant extract functioned as natural capping and stabilising agents, facilitating the formation of Co_3O_4 nanoparticles under meticulously controlled conditions. The Rietveld refinement of XRD patterns substantiated the synthesis of cobalt oxide nanoparticles exhibiting a cubic crystal structure. The elastic behaviour of Co_3O_4 nanoparticles, influenced by various components of Eichhornia crassipes, exhibits notable variation. The elastic moduli of Co_3O_4 nanoparticles enhanced with stem are measured at 176.58, 65.91, and 183.40 GPa, representing the highest values when compared to those of Co_3O_4 nanoparticles enhanced with leaf and root. Among the samples examined, the one enhanced by leaf assistance exhibited the most diminutive crystallite size, measuring at 12.5 nm. The FT-IR analysis substantiated that the metal-oxygen vibrations beneath 1000 cm^{-1}, evidenced by peaks at 650 cm-1 and 537 cm^{-1}, affirmed the successful synthesis of Co_3O_4 NPs featuring both tetrahedral and octahedral Co–O bonding. The analysis of Co_3O_4 nanoparticles was conducted through UV-Visible diffuse reflectance spectroscopy (DRS), revealing direct band gap energies of 3.29 eV, 3.37 eV, and 3.28 eV. A relationship was identified between particle size and band gap energy, indicating that larger particles (18.90 nm) displayed a reduced band gap (3.28 eV). The analysis of photoluminescence substantiated the energy band gap and optical characteristics of Co_3O_4 nanoparticles. The FE-SEM analysis indicated a spherical morphology characterised by agglomeration for the Co_3O_4 nanoparticles assisted by leaves and stems, while those facilitated by roots displayed porous, dispersed spherical structures. The EDX analysis substantiated the synthesis of Co_3O_4 nanoparticles through the identification of significant peaks associated with cobalt (Co) and oxygen (O). The zeta potential measurements for cobalt oxide nanoparticles revealed negative values of -41.9 mV for leaves and -40.1 mV for roots, thereby affirming their commendable colloidal stability.

Keywords: Green Synthesis, Cobalt Oxide Nanoparticles (Co_3O_4), Eichhornia Crassipes, Rietveld Refinement, Optical Band Gap, Zeta Potential.

1. Introduction

The tricobalt tetra-oxide (Co_3O_4) is a multipurpose transition metal oxide which has been widely used in Li-ion batteries as an anode material, high-temperature solar selective absorbers, sensors, photocatalysts, supercapacitors, etc [1, 2]. The crystal structure of (Co_3O_4) is isometric to the magnetite Fe_3O_4 and is *p*-type semiconductor with paramagnetic behaviour at room temperature [3]. In Co_3O_4, the Co^{2+}/Co^{3+} ions occupy tetrahedral (*A*) and octahedral (*B*) sites [3]. The magnetic nature of Co_3O_4 can depend on the role of magnetic Co^{2+} while Co^{3+} is non-magnetic. The magnetic Co^{2+} ($3d^7$) ions with high spin (S = 3/2) occupy *A*-sites while non-magnetic Co^{3+} ($3d^6$) ions with low spin (S = 0) occupy *B*-sites. The non-magnetic Co^{3+} ions have paired *d* electrons and does not contribute to the magnetic nature. The magnetic Co^{2+} ions have three

unpaired *d* electrons and are not ordered at room temperature which leads to paramagnetic nature of Co_3O_4 above Néel's temperature (T_N) 30 K [4]. Below the T_N, overwhelms the paramagnetic behaviour and resulted to the antiferromagnetic behaviour due to ordering between the Co^{2+} ions.

The outlook of Co_3O_4 in nanometric scale dimensions, scaled its uniqueness due to finite-size effects, formation of the inverse spinel structure, uncompensated surface spins and so on [5, 3]. Different wet-chemical methods like co-precipitation method [6], hydrothermal method [7], thermal decomposition [8], sonochemical process [9], microemulsion method [10], sol-gel method [11] and so on have been reported to synthesis Co_3O_4 nanoparticles. However, the hazardous gases liberated during these processes due to utilization of synthetic chemicals are uncontrollable. Moreover, these gases are harmful to the humans and surrounding environment. To control these raised factors, an ecofriendly green synthesis methods are frequently adopting. Mohammadi *et al.* [12], synthesized Co_3O_4 nanoparticles using walnut green skin extract. They observed that the prepared cobalt oxide nanoparticles are superparamagnetic in nature. They reported four optimum parameters like cobalt nitrate (50 mmol), extract volume (10 ml), time (92 min) and temperature (53^{o}C) to obtain Co_3O_4 phase using green synthesis method. Khalid *et al*. [13], prepared Co_3O_4 nanoparticles by employing green chili and sunflower seeds extracts useful for capacitive electrode material. They confirmed the metal oxide phase from the XRD and FTIR analysis. They obtained 1080.32 F/g specific capacitance and 86.70% capacitance retention at higher scan rate of10 A/g. Diallo *et al.* [14], obtained Co_3O_4 nanoparticles using Aspalathus linearis leaf extract. They reported surface/interface and optical properties. They obtained a particle size ~3.6 nm with the reticular atomic plans under a slight compressive state. Dewi *et al*. [15] produced Co_3O_4 nanoparticles using Euphorbia heterophylla L. leaves extract. They reported good photocatalytic activity of Co_3O_4 in the degradation of methylene blue about 63.1% for 3 h.

Summarizing the cited reports, different plant extracts have been successfully utilised to produce Co_3O_4 nanoparticles in green synthesis approaches. In our previous studies [16], we used natural fuels like wine, honey and cow-urine to prepare Co_3O_4 nanoparticles using sol-gel auto-combustion method. We successfully implemented ecofriendly green synthesis approach and prepared Co_3O_4 nanoparticles. The obtained nanoparticles showed excellent antibacterial behaviour. To the best of our knowledge, the preparation of Co_3O_4 nanoparticles using different parts of Eichhornia crassipes (water hyacinth) in the green synthesis method have not been found. The possible reason for considering Eichhornia crassipes (water hyacinth) is that it contains rich of acids like gallic acid ($C_7H_6O_5$), caffeic acid ($C_9H_8O_4$), ferulic acid ($C_{10}H_{10}O_4$) and chlorogenic acid ($C_{16}H_{18}O_9$). These acids can be acted as caping agents and easily probe the ignition for auto-combustion along with the urea in the synthesis process. In the present study, Co_3O_4 nanoparticles are synthesized by eco-friendly green synthesis approach using extracts of Eichhornia crassipes. The obtained powders are characterized for various studies.

2. Experimental Method

2.1. Materials

Analytical grade cobalt (II) nitrate hexahydrate (Co $(NO_3)_2.6H_2O$) and Urea $((H_2N)_2CO)$ chemicals were purchased to synthesize the cobalt oxide nanoparticles. The double-distilled water was used throughout the experiment.

2.2. Method of Preparation

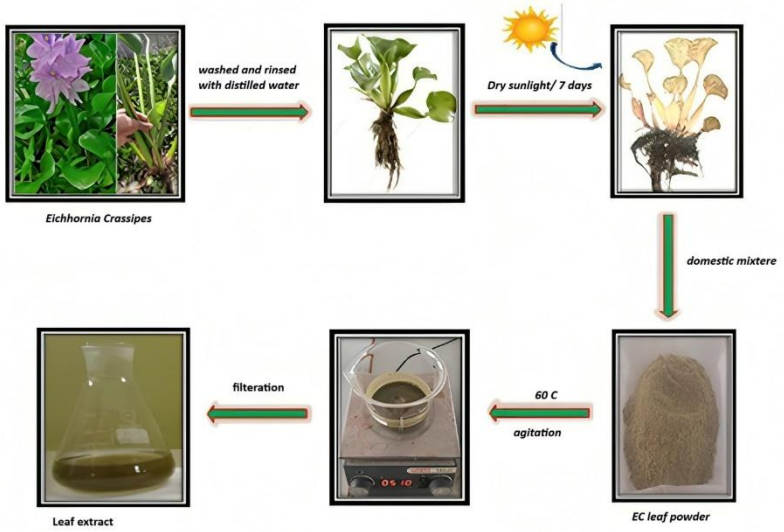

Figure 1. Preparation of Eichhornia crassipes leaf extract

2.2.1. Preparation of Eichhornia Crassipes Leaf, Stem and Root Extract

Eichhornia crassipes, popularly known as water hyacinth, was collected from Annur, Coimbatore, Tamil Nadu, and India. The plant leaves, stem and root were separated and first washed with tap water several times to remove the dirt and other contaminations. This was further rinsed in distilled water and allowed to dry in the sunlight for seven days. Then, the individual dried plant materials were crushed and powdered using a domestic mixer. In this present work, the aqueous extract was prepared by adding 7.2 g of the powdered *Eichhornia crassipes* leaf immersed in 150 ml of double-distilled water in a beaker. The mixture was heated at 60 ºC and agitated continuously for an hour, and the volume was reduced by half. Then, the extract was cooled at room temperature and filtered using Whatman No. 1 filter paper. The aqueous leaf extract was used for further analysis. The same procedure was continued to prepare stem and root extracts. Figure 1. Shows the preparation of *Eichhornia crassipes* leaf extract.

2.2.2. Chemical Synthesis of Cobalt Oxide Nanoparticles

A solution was prepared by adding 14.56 g of cobalt nitrate hexahydrate (1M) crystals mixed with 50 ml of double-distilled water (as a solvent). The urea salt (3.65 g) was added (as a fuel) to the above solution. The mixture was kept under constant stirring for an hour to obtain a clear, homogeneous solution. Then, the prepared 50 ml of aqueous leaf extract (as a capping agent) was added drop by drop with constant stirring under a magnetic stirrer to the homogeneous solution. The resulting solution is placed in a hot plate heater. The temperature was maintained at 130 ºC for twenty minutes. Initially, the mixture is boiled, and it undergoes a combustion reaction. The ultimate desiccated residue was collected and powdered using an agate motor pestle to obtain leaf cobalt oxide NPs. The synthesis procedure was also conducted to prepare the stem and root of cobalt oxide NPs. The various strategies were employed to analyze the physicochemical behavior of the fine powders using different characterization techniques.

2.3 Characterization techniques

- All the prepared cobalt oxide powdered samples are examined using a Bruker D8 Advance X-Ray Diffractometer (λ = 1.5406 Å) to explore the structural properties.
- Fourier transform Infrared Spectroscopy (FT-IR), JASCO-4700 Spectrometer, was employed to identify the chemical bond structure of the NPs.
- To determine the energy band gap of the prepared Co_3O_4 nanoparticles using UV-VISIBLE NIR (V-770) Spectrophotometer.
- The Photoluminescence (PL) studies JASCO FP-8250 were conducted to investigate the optical properties of the Co_3O_4 nanoparticles.
- A JEOL 5600 LV scanning electron microscope at an accelerating voltage of 10 kV was employed to study the morphology of the sample through SEM pictures and compositional analysis through EDX.
- The stability of the colloidal nanoparticles (NPs) was evaluated using a Horiba SZ-100 zeta potential analysis technique.

3. Result and Discussion

3.1 XRD Analysis

X-ray diffraction (XRD) was used to analyze the crystalline structure of synthesized nanoparticles from *Eichhornia Crassipes* (EC*)* plant parts (leaf, stem and root). This non-destructive technique provided valuable information on phase composition and structural properties. The XRD patterns of EC-leaf, EC-stem and EC-root are depicted in Figure 2.

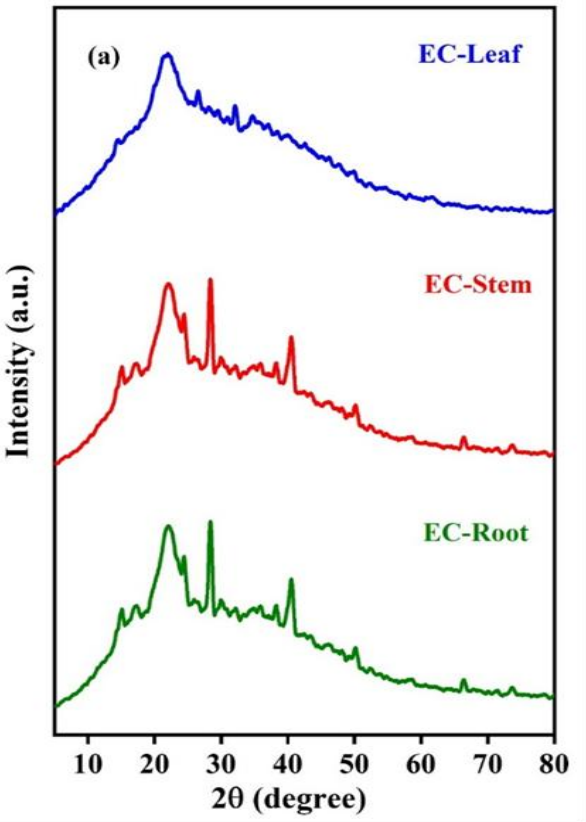

Figure 2. XRD patterns of Eichhornia crassipes (EC) leaf, stem and root

The patterns exhibited the crystalline and amorphous characteristics. The diffraction peaks observed at 15.2º and 22.5º correspond to (101) and

(002) lattice planes which are commonly available peaks for EC. The presence of diffraction peaks is ascribed to the crystalline nature of water hyacinth which is due to the cellulose presence. Similar type of XRD reports for EC can be found in the literature [17]. The Rietveld refined XRD patterns of the synthesized Co_3O_4 samples assisted with leaf, stem and root of *Eichhornia crassipes* (EC) are shown in Figure 3. The X-ray diffractograms were analysed using Profex software and the results confirm the formation of single-phase cubic spinel structure without any detectable impurity peaks. The quality of refinement was evaluated based on the goodness of fit (GoF) and the chi-squared (χ^2) values. For R-Co_3O_4, the refinement yielded GoF = 1.3 and χ^2 = 1.68, indicating an excellent match between the observed and calculated patterns. Similarly, S-Co_3O_4 showed GoF = 1.56 and χ^2 = 2.43, while L-Co_3O_4 exhibited GoF = 1.6 and χ^2 = 2.14, both reflecting reliable refinement quality within acceptable limits. These values suggest that the refinement procedure was successful for all 3 samples, with minor variations attributed to differences in crystallite size, micro-strain and morphology. The refinement results validate the structural integrity and phase purity of the Co_3O_4 samples. The lattice parameter is evaluated from the Rietveld refinement analysis and is denoted as *a′*. The values of *a′* along with refinement parameters are listed in Table.1. The XRD pattern exhibits prominent peaks at 2θ values of 19.04º, 31.3º, 36.89º, 44.9º, 59.4º, and 65.3º, corresponding to the specific lattice planes (111), (220), (311), (400), (511) and (440). These diffraction peaks are consistent with the JCPDS No. 76–1802 [18]. The extra peaks have not been found in the patterns indicating phase purity of Co_3O_4 nanoparticles. The bio-molecules from the parts of EC matted the strings with the cobalt sources to coagulate the nucleation among cobalt and oxygen sites due to electron donor of bio-molecules to form Co_3O_4 phase. Similar studies can be found in the literature [19]

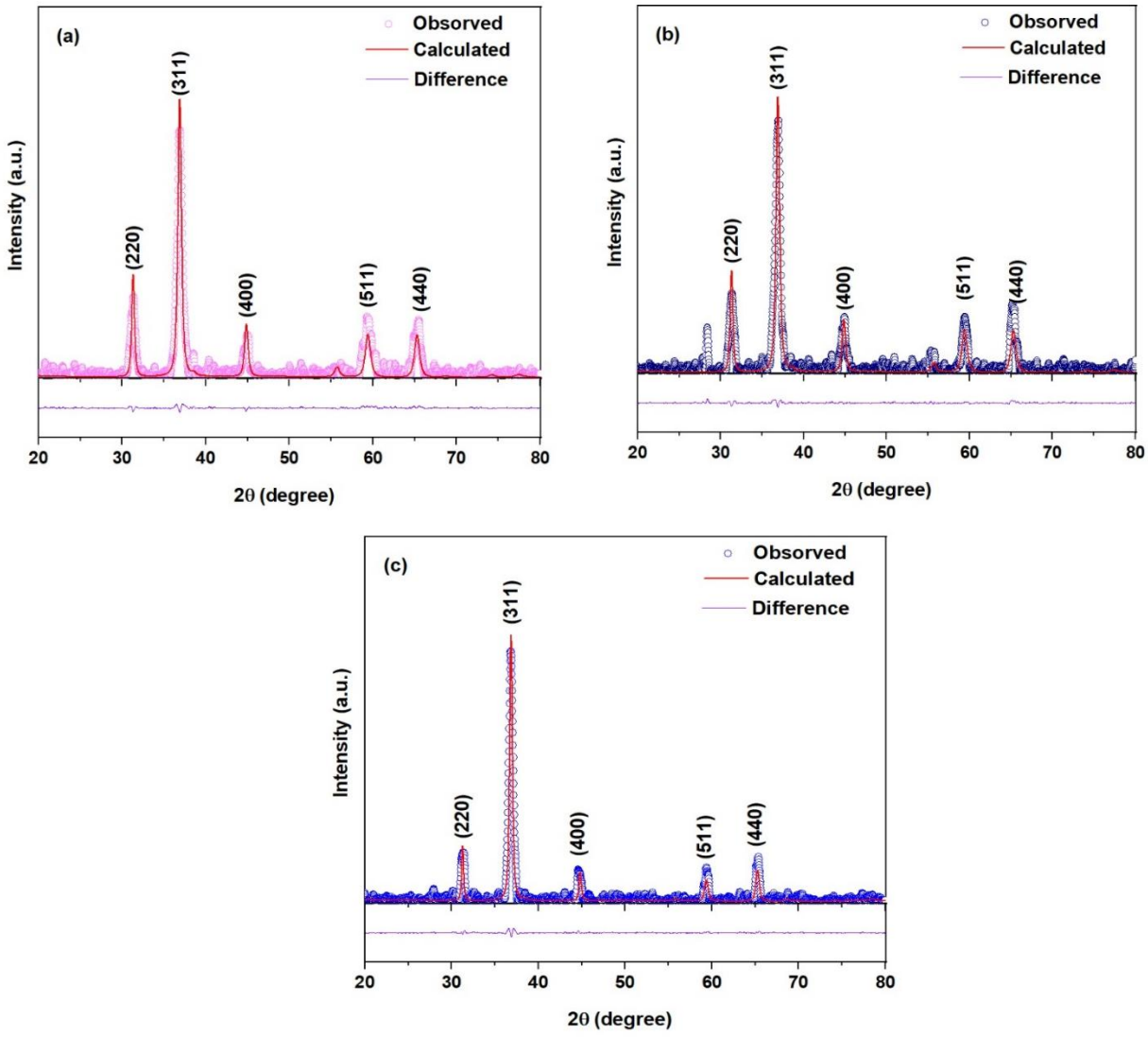

Figure 3. Rietveld refined XRD patterns of **(a)** L-Co3O4 **(b)** S-Co_3O_4 and **(c)** R-Co_3O_4 NPs.

Table. 1. Rietveld refinement parameters along with lattice parameter.

Sample	a´ (Å)	R_w	R_{exp}	GoF	χ^2
L-Co_3O_4	8.08820	3.3	3.0	1.6	2.14
S-Co_3O_4	8.08600	3.9	3.2	1.56	2.43
R-Co_3O_4	8.08830	4.0	2.6	1.3	1.68

Table.2. Structural characteristics of Co_3O_4 NPs synthesized using leaf, stem, and root extracts.

Sample	Crystalline size *D* (nm)	Lattice parameter *a"* (Å)
L-Co_3O_4	12.5	8.068
S-Co_3O_4	13.8	8.070
R-Co_3O_4	18.9	8.080

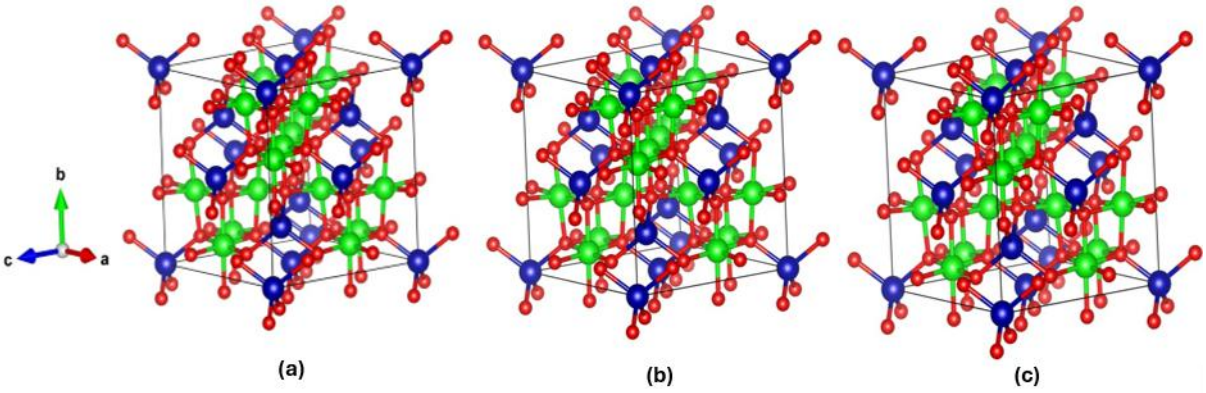

Figure 4. Structure of **(a)** L-Co_3O_4, **(b)** S-Co_3O_4 and **(c)** R-Co_3O_4 NPs.

The lattice parameter (*a*) has been calculated from X-ray diffraction data using the formula [4].

$$a = d_{(hkl)}\sqrt{h^2 + k^2 + l^2} \quad (1)$$

Where $d_{(hkl)}$ = interplanar spacing between (*hkl*) planes and *h*, *k*, *l* = Miller indices.

The average crystalline size (*D*) was calculated by using the Debye Scherrer formula [20].

$$D = \frac{k \cdot \lambda}{\beta \cdot \cos\theta} \quad (2)$$

Where *k* = shape factor, λ = wavelength of X-ray beam, β = full width at half maximum, θ = Bragg's angle of diffraction.

The lattice parameter evaluated using the Eq.(1) is denoted as *a*". The values of *a*" and *D* are summarized in Table 2. The values of *a*′ and *a*" are consistent with each other. The present values of lattice parameter are consistent with the reported values in the literature [21]. It can be observed that the lattice parameter of Co_3O_4 NPs prepared assisted with leaf is lower than the lattice parameter of Co_3O_4 NPs assisted with stem and root. Such variation of lattice parameter is due to changes in bond length of Co^{3+}-O^{2-} ion complex which depend on occupancy of Co^{3+} ions in the spinel network. The occupancy of cobalt ions in the spinel network of Co_3O_4 NPs is shown in Figure 4. In all samples, the spinel lattice is preserved with Oxygen anions (red solids) form the cubic close-packed framework. Co^{2+} (blue solids) exclusively occupies one-eighth of tetrahedral (*A*) sites while Co^{3+} (green solids) occupies half of the octahedral (*B*) sites, yielding the normal spinel distribution $(Co_1^{2+})_{tetra}[Co_2^{3+}]_{octa}O_4$ [22]. In order to maintain charge neutrality, some of the Co^{3+} ions replaced Co^{2+} ions in the spinel network. Such an occupancy alters the bond lengths of Co^{2+}-O^{2-} and Co^{3+}-O^{2-} ion complexes resulting to changes in the lattice parameter. However, the spinel topology is preserved across the three samples. Finally, the differences in precursor chemistry are expected to influence crystallite size, surface defects and surface chemistry rather than the fundamental cation ordering. The sharp and intense peaks suggest a high degree of crystallinity in the prepared Co_3O_4 NPs. These characteristic peaks confirm the formation of cobalt oxide nanoparticles with a cubic crystal structure. Here in the leaf assisted synthesized nanomaterial exhibited the least crystallite size of 12.5 nm. The growth of crystallite can be expected due to the liberation of thermal energy from the rate of combustion reaction between metal compounds and bio-molecular interaction change of parts of EC.

3.2 Mechanical behaviour analysis

The 2D and 3D plots of elastic properties such as Young's modulus (E), Shear modulus (G), and Poisson's ratio (v) for Co_3O_4 derived from Eichhornia crassipes leaf (L), root (R), and stem (S) are shown in Figure.5, Figure.6 and Figure 7. The elastic properties determined by Voigt approximation are given in Table 3. In the 2D projections, blue and green regions indicate the maximum and minimum values, respectively, while the 3D contours display the spatial anisotropy of the elastic response.

Table 3. Elastic properties of Co_3O_4 NPs.

Sample	E (GPa)	G (GPa)	B (GPa)	v	B/G
L-Co_3O_4	131.96	47.85	181.82	0.379	3.8
	Anisotropy				
	2.16	2.315	-	3.6873	2.8
S-Co_3O_4	176.58	65.91	183.4	0.339	
	Anisotropy				
	1.055	1.062	-	1.123	2.8
R-Co_3O_4	170.79	63.69	178.87	0.386	
	Anisotropy				
	1.075	1.084	-	1.168	

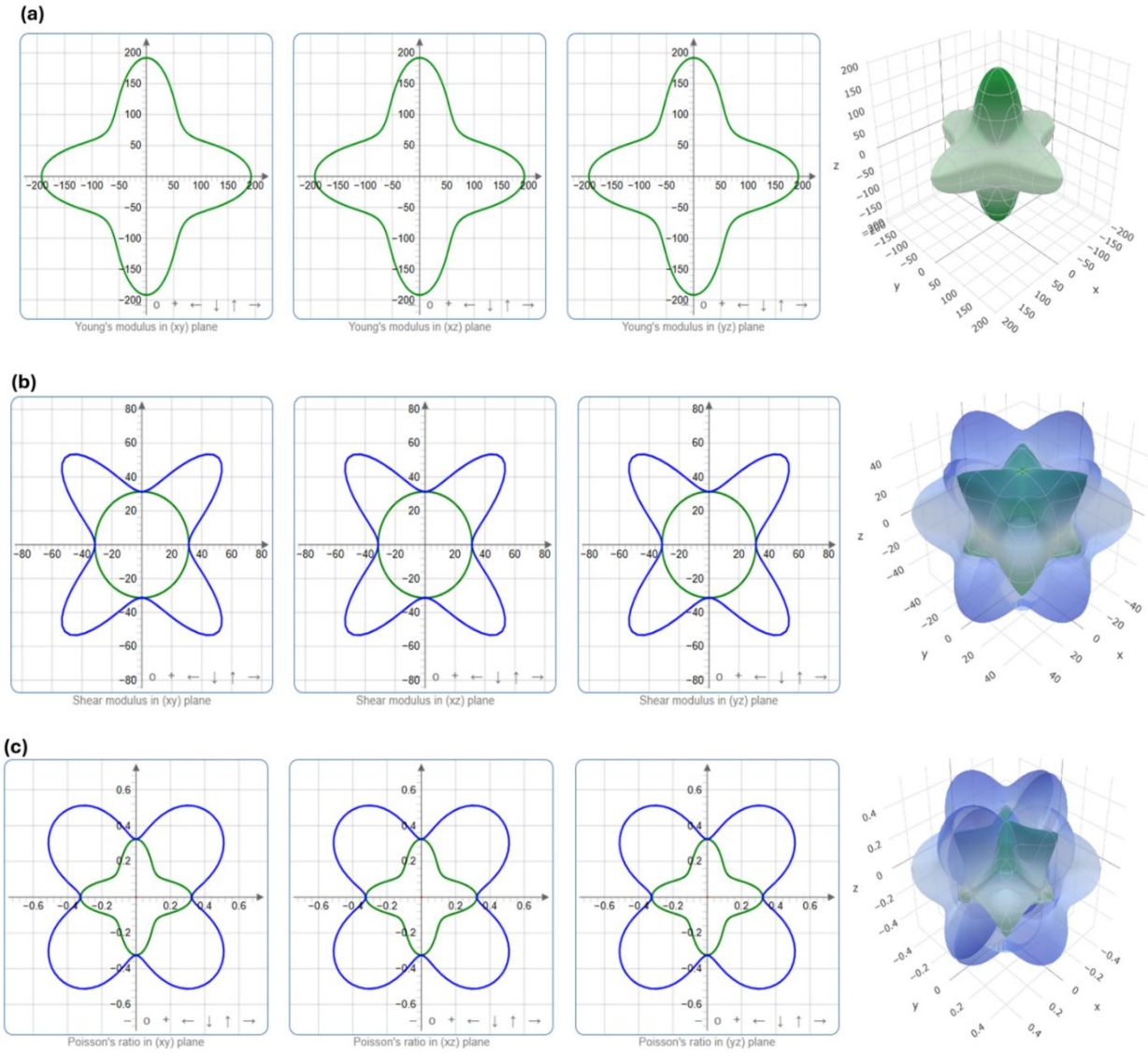

Figure 5. 2D and 3D illustration of variation of **(a)** E, **(b)** G and **(c)** v along different crystallographic axes for L-Co_3O_4.

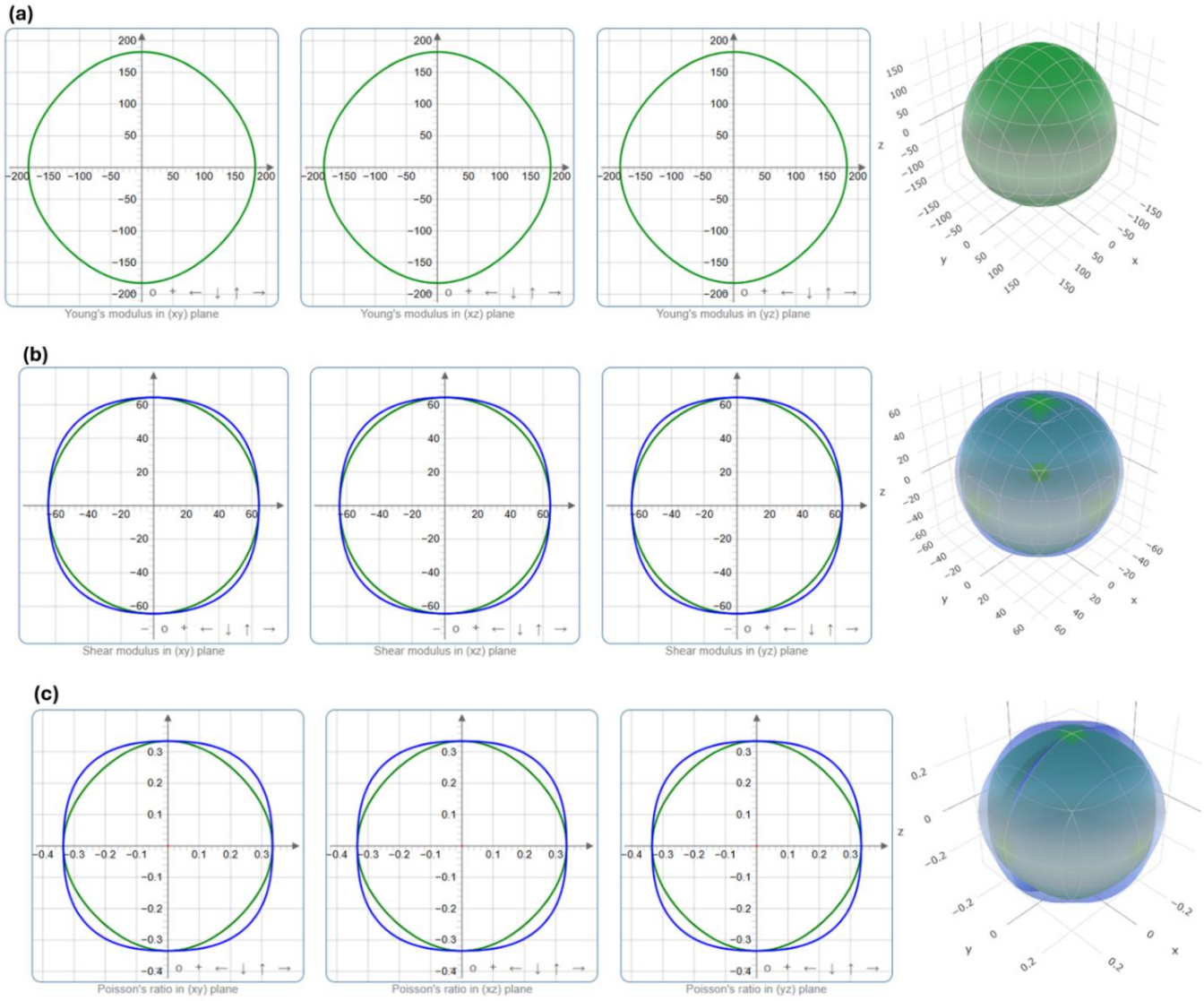

Figure 6. 2D and 3D illustration of variation of **(a)** E, **(b)** G and **(c)** along different crystallographic axes for S-Co_3O_4.

Among the three samples, S-Co_3O_4 exhibits the highest Young's modulus (176.58 GPa) and shear modulus (65.91 GPa), indicating higher stiffness and rigidity.

L-Co_3O_4 shows the lowest values (E = 131.96 GPa, G = 47.85 GPa), indicating a comparatively softer nature. Bulk modulus (B) remains nearly similar (~179–183 GPa) across all samples, indicating that compressibility is minimally affected by fuel type. Poisson's ratio (v) varies from 0.34 in S-Co_3O_4 to 0.39 in L-Co_3O_4, suggesting that the leaf-derived Co_3O_4 has higher lateral strain under load consistent with its lower stiffness. Anisotropy values further confirm that L-Co_3O_4 is evidently anisotropic (2.16 for E, 2.31 for G and 3.69 for v) whereas R- and S-Co_3O_4 exhibit nearly isotropic nature (anisotropy ≈1.05–1.17). These results highlight that the plant part used in the bio-combustion significantly influences the mechanical performance of Co_3O_4. The variation of elastic moduli in Co_3O_4 NPs assisted with different parts of Eichhornia crassipes can also be expected due to changes in the bond lengths of Co^{2+}-O^{2-} and Co^{3+}-O^{2-} ion complexes. These results support the structural features of Co_3O_4 NPs. The Pugh's ratio (B/G), which is an important indicator of ductile–brittle behaviour, was calculated for different Co_3O_4 samples (see Table 3). L-Co_3O_4 exhibits the highest value (≈3.8), while R- and S-Co_3O_4 exhibited comparatively lower but still high ratios (≈2.8). Since B/G>1.75 is generally associated with ductility, all three variants can be considered ductile, with L-Co_3O_4 showing the greatest resistance to shear-induced fracture. These results evident that the choice of plant precursor modulates the balance between stiffness and toughness in bio-templated Co_3O_4.

3.3. FT-IR analysis

The Fourier Transformation Infrared (FT-IR) spectroscopy was utilized to investigate the functional groups and vibrational patterns present in the nanomaterials. The FT-IR recorded in range (4000-400 cm^{-1}) for the powdered leaf, stem and root of *E. crassipes* is shown in Figure 8.

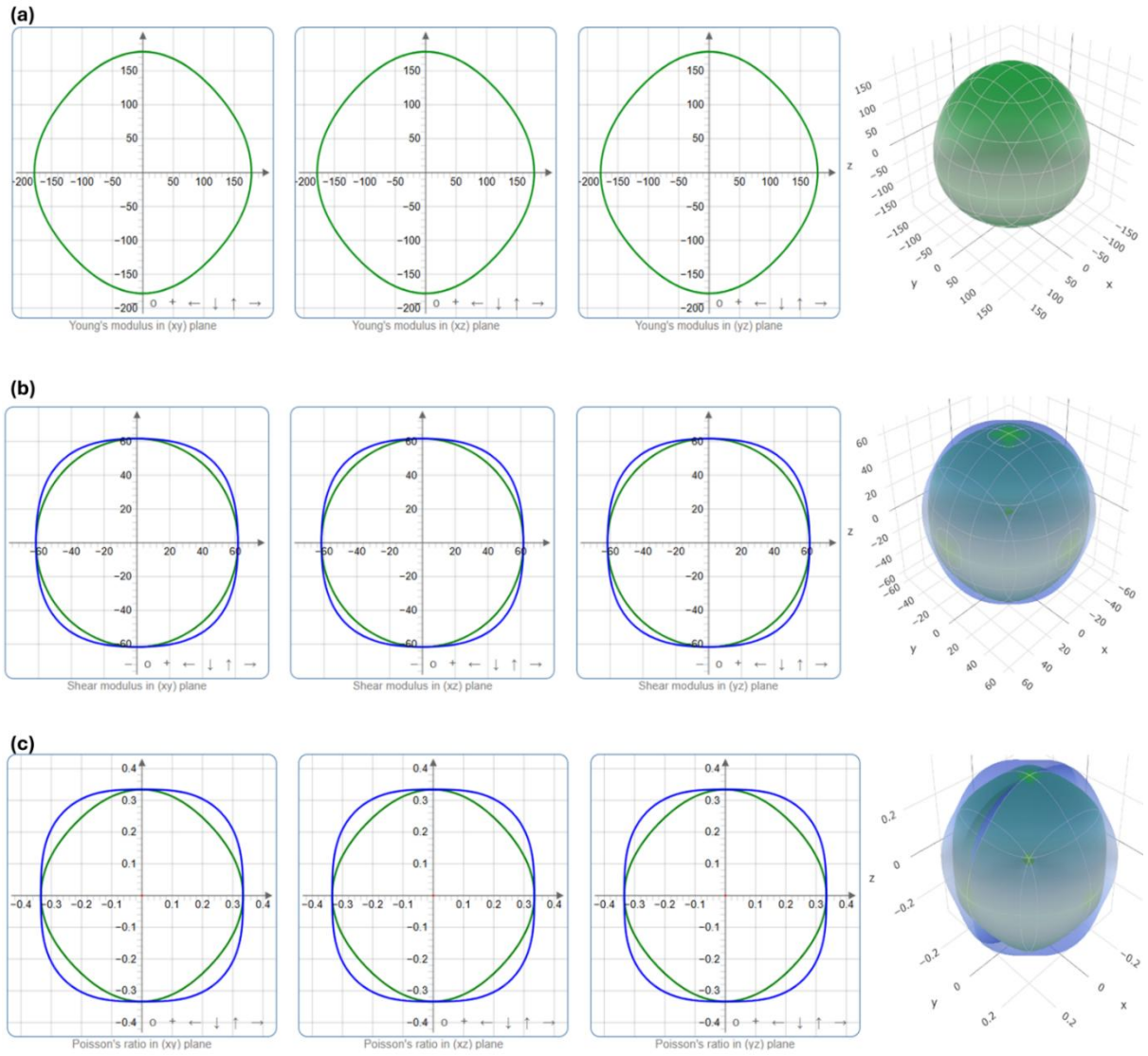

Figure 7. 2D and 3D illustration of variation of **(a)** E, **(b)** G and **(c)** v along different crystallographic axes for R-Co_3O_4.

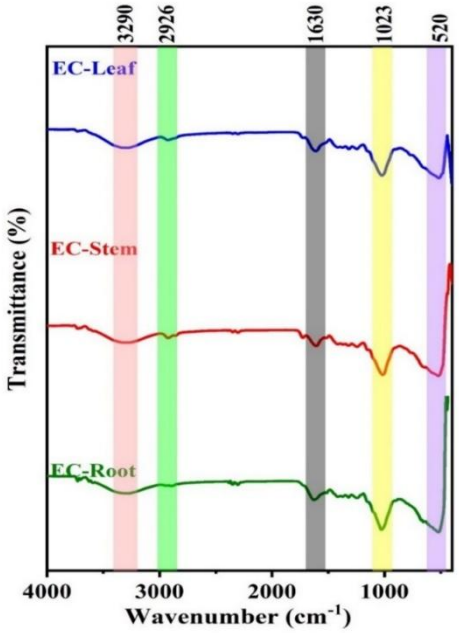

Figure 8. FT-IR spectra of powdered E. crassipes: **(A)** leaf, **(B)** stem, and **(C)** root

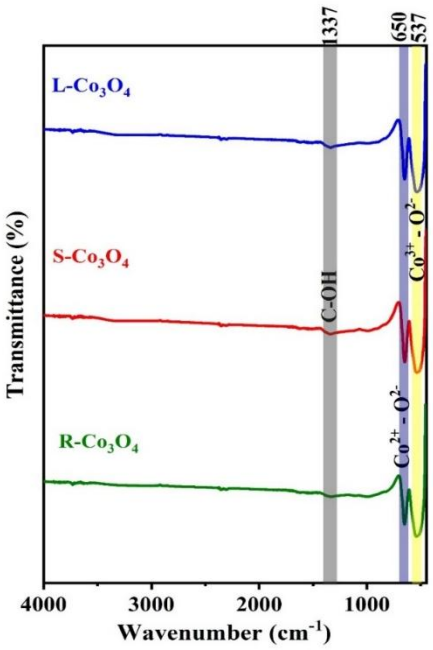

Figure 9. Shows the FT-IR spectra of plant extracts mediated Co_3O_4 NPs.

It revealed distinct absorption bands indicating the presence of various functional groups. A broad band at 3290 cm^{-1} is attributed to O-H stretching vibrations in hydroxyl groups. The absorption band at 2926 cm^{-1} was attributed to asymmetric alkane C-H stretching vibrational modes. The band absorbed at 1630 cm^{-1} owing to the C=O stretching, the presence of esters, and carboxylic acids. The strong peak was observed at 1023 cm^{-1} which is assigned to the C-O of ester and ethers. The peak at around 537 cm^{-1} corresponds to the C-X stretching vibrations of alkyl halides [23]. The range of the FT-IR spectra of plant extracts mediated Co_3O_4 NPs was recorded in the range of 4000-450 cm^{-1} shown in Figure 9. The tiny peak at 1337 cm^{-1} is responsible for the C-OH functional group. The two distinct peaks absorbed at 650 and 537 cm^{-1} were attributed to the stretching vibrations of Co^{2+}-O^{2-} in tetrahedral coordination and Co^{3+}-O^{2-} in octahedral coordination, respectively. The peaks below 1000 cm^{-1} corresponded to the characteristic vibrational frequencies of metal oxide [24, 25].

3.4. UV-Vis spectroscopy analysis

UV-Visible diffuse reflectance spectroscopy (DRS) was employed to investigate the optical characteristics of Co_3O_4 nanoparticles synthesized using different parts of the *Eichhornia crassipes* plant, including leaf, stem, and root extracts. The optical properties of these synthetic materials provide valuable insights into their energy bandgap and excitonic transitions. The UV-Vis spectra of the three synthesized nanoparticles are shown in Figure.10 (a-c). A broad absorption peak ranging from 200-370 nm can be observed from the spectra. Using Tauc's relation the direct band gap energy (E_g) values of Co_3O_4 NPs are evaluated [26].

$$(ahv)^n = A.(hv - E_g) \quad (3)$$

where α = absorption coefficient, hu = photon energy, A = constant and n = type of optical transition.

The value of n depends on the nature of transition. For indirect allowed transition n = 2, for direct allowed transition n = 1/2, for direct forbidden transition n = 3/2 and n = 3 for indirect forbidden transition [27]. The corresponding Tauc plots are shown in Figure 10 (d-f). The optical band gap energy values have been determined by extrapolating the linear region of the Tauc plot graph that was drawn between hu vs $(ahu)^2$ [28]. This indicates that the synthesized Co_3O_4 NPs have optical band gap of 3.29, 3.37 and 3.28 eV respectively. This revealed, the decrease of optical band gap energy with an increase in particle size, the nanoparticle having the largest particle size (18.9 nm) resulted in the lowest band gap energy of 3.28 eV.

3.5 Photoluminescence Analysis

The photoluminescence (PL) spectrum of Co_3O_4 NPs reveals two distinct peaks in the UV region. The PL emission spectra of cobalt oxide (Co_3O_4) nanoparticles was absorbed at 200-600 nm as excitation wavelength is shown in Figure.11. This obtained a broad spectrum as a result of emission in the range 220-430 nm, accompanied by two peaks at 320 nm and 385 nm with band gap values of 3.22 eV, 3.18 eV, and 3.21 eV for L-Co_3O_4, S-Co_3O_4, and R-Co_3O_4 NPs respectively. These are close with the reported values in the literature [29].

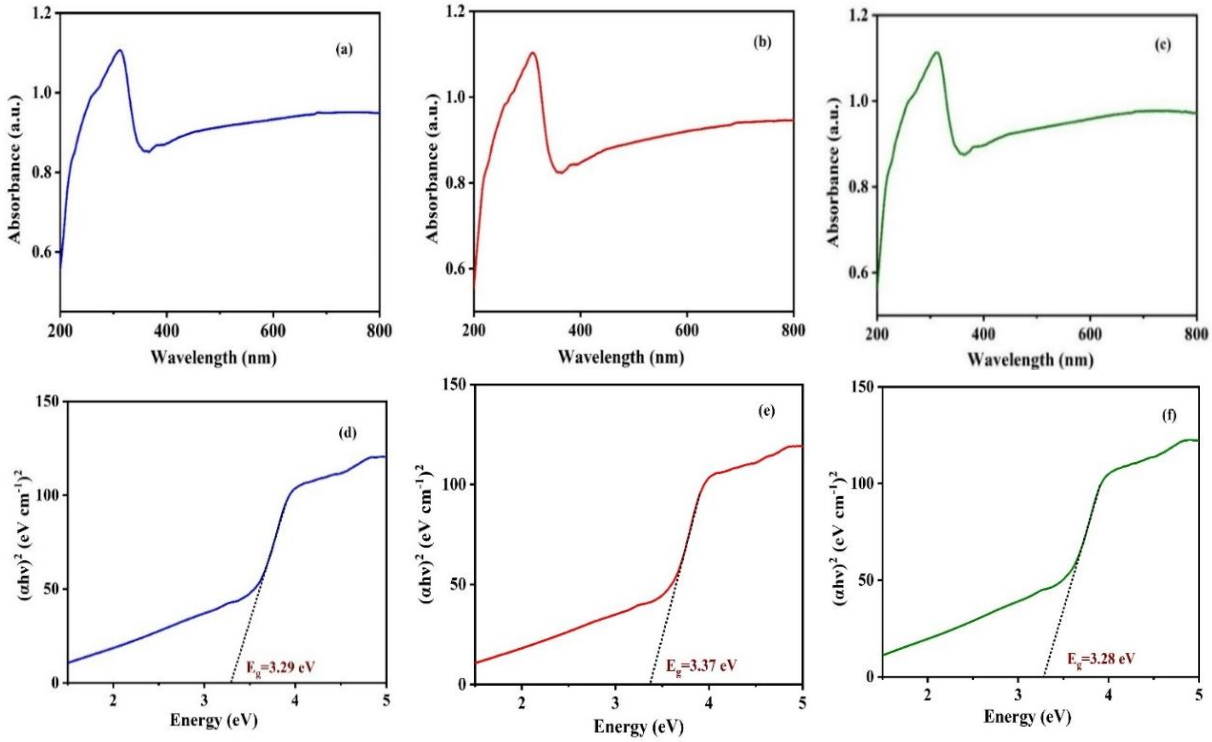

Figure 10(a-c). UV-Vis absorption spectra and **(d-f):** Tauc plots of Co_3O_4 nanoparticles synthesized using different parts of the Eichhornia crassipes

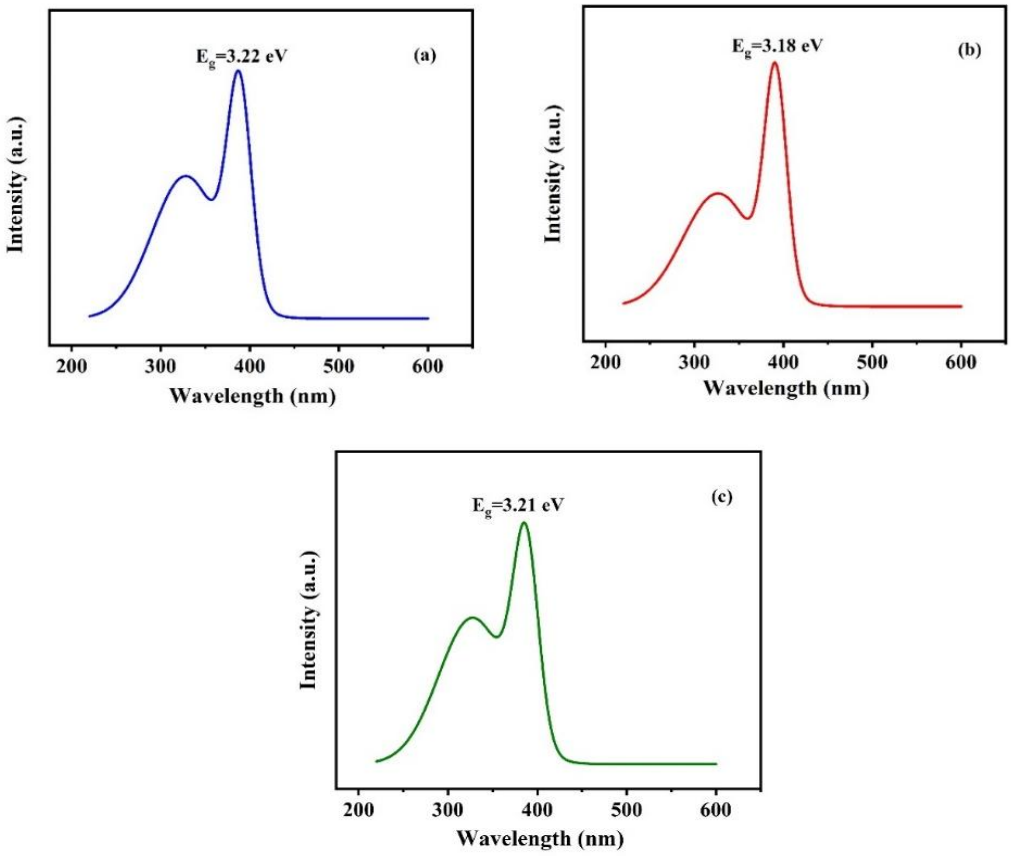

Figure 11. Shows the PL emission spectra of **(a)** L-Co_3O_4, **(b)** S-Co_3O_4 and **(c)** R-Co_3O_4 NPs.

3.6 Surface Morphology Analysis

Field Emission Scanning Electron Microscopy (FE-SEM) analysis investigated the surface morphology of Co_3O_4 nanoparticles synthesized by combining different parts of the *Eichhornia crassipes* plant. Figure.12, showed the FE-SEM images of Co_3O_4 NPs at different magnifications and revealed the regular spherical morphology with agglomeration for cobalt oxide nanoparticles assisted with leaf and stem extract whereas the morphology of root assisted cobalt oxide nanoparticles exhibited visible pores with spherical particles scattered throughout its surface.

3.7 EDX analysis

Energy-Dispersive X-ray (EDX) analysis was performed to determine the elemental composition of the synthesized Co_3O_4 NPs. The respective images are as shown in Figure. 13 along with the elemental composition. The presence of prominent peak in the EDX spectrum for Cobalt (Co) and Oxygen (O) was observed on the synthesized nanoparticles assisted with leaf, stem and root of extracts confirmed the formation of cobalt oxide NPs. However, some minor peaks also appear, indicating the presence of Carbon (C), Sodium (Na), Potassium (K), Magnesium (Mg), and Chlorine (Cl), which was attributed due to the residual components of the *Eichhornia crassipes* plant extract.

3.8 Zeta Potential Analysis

The absolute value of zeta potential can be used to determine the colloidal stability of the synthesized Co_3O_4 nanoparticles, as shown in Figure.14. The zeta potential measurements revealed that the *Eichhornia crassipes*-assisted Co_3O_4 NPs, prepared using leaf, stem and root extracts, exhibited zeta potential values of -41.9 mV, -22.5 mV, and -40.1 mV, respectively.

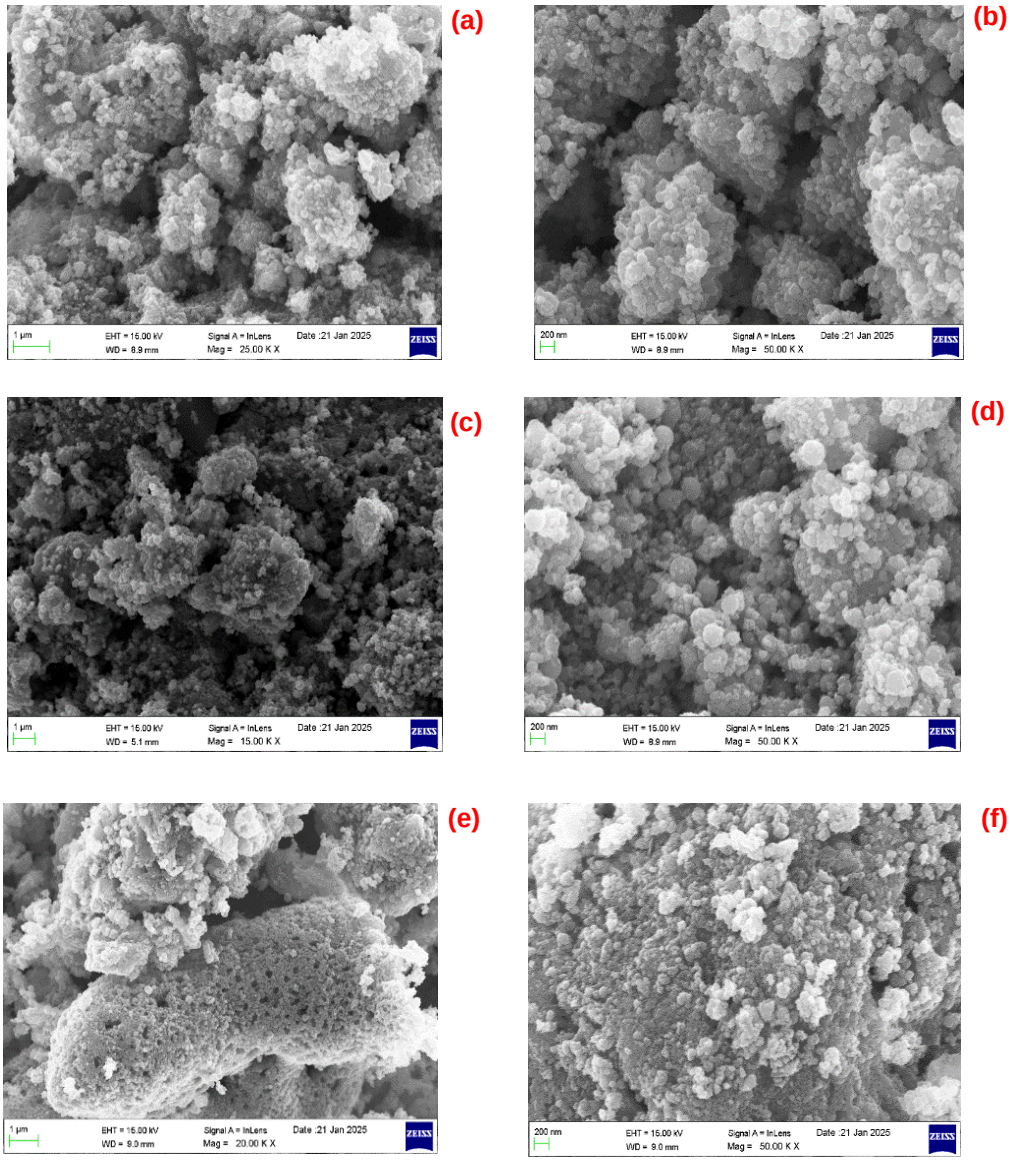

Figure 12. FE-SEM images of **(a, b)** L - Co_3O_4, **(c, d)** S - Co_3O_4, **(e, f)** R - Co_3O_4

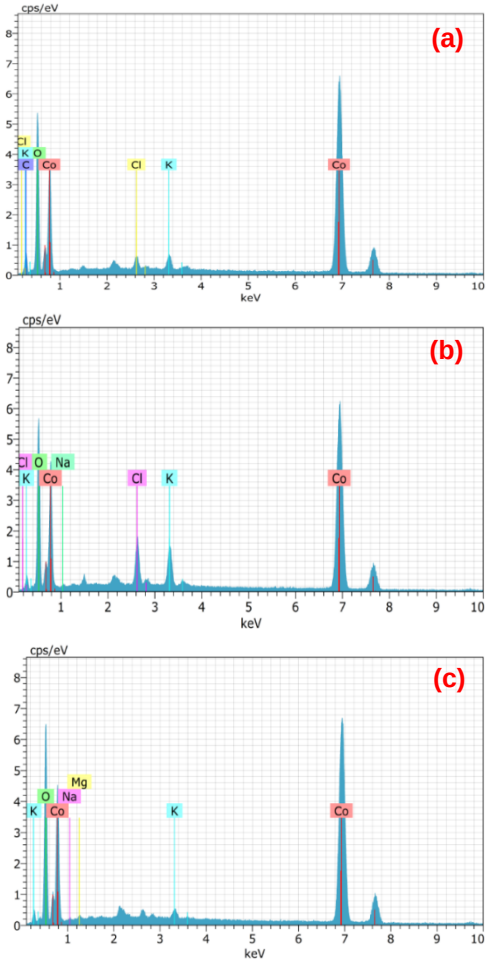

Element	Wt%	Atomic %
Co	67.93	35.75
O	23.37	45.3
C	6.83	17.64
K	0.97	0.77
Cl	0.62	0.54

Element	Wt%	Atomic %
Co	62.94	39.15
O	23.79	54.5
K	2.94	2.76
Cl	2.74	2.84
Na	0.48	0.76

Element	Wt%	Atomic %
Co	68.27	44.19
O	22.58	53.83
K	0.58	0.57
Na	0.46	0.76
Mg	0.41	0.64

Figure 13. (a-c) EDX images and corresponding elemental mapping tables of Co_3O_4 NPs synthesized using **(a)** leaf, **(b)** stem, and **(c)** root extracts of Eichhornia crassipes plant.

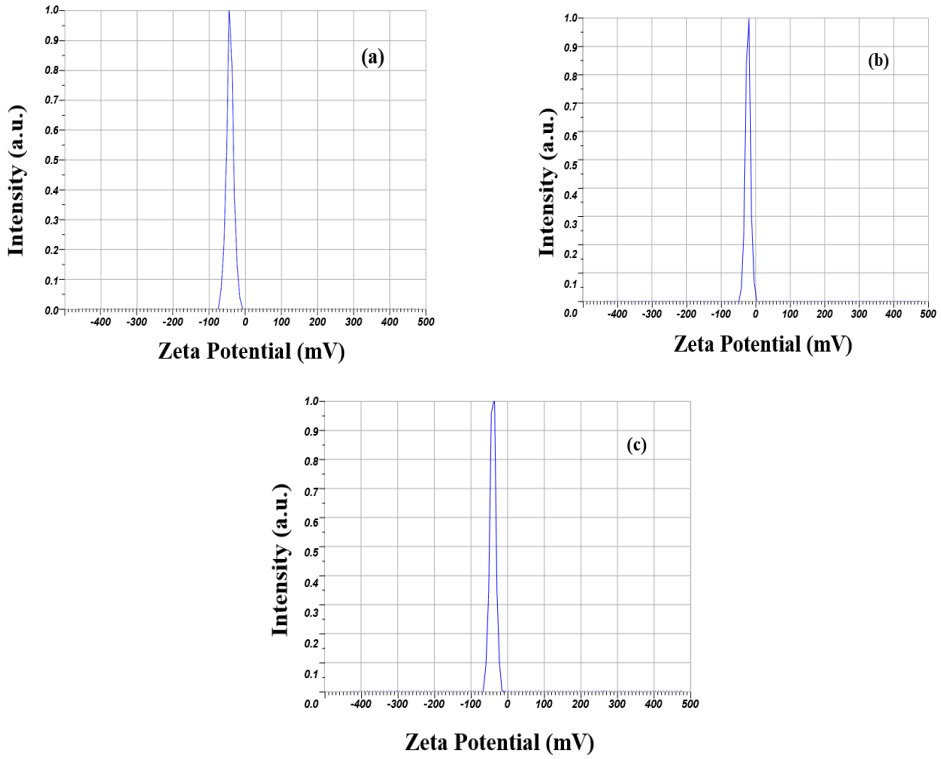

Figure 14. Zeta potential analysis of **(a)** L-Co_3O_4, **(b)** S-Co_3O_4, and **(c)** R-Co_3O_4 NPs.

The high negative zeta potential values of the leaf and root extract-mediated Co_3O_4 NPs indicate a strong electrostatic repulsion between particles, resulting in enhanced stability and reduced particle agglomeration. In contrast, the lower zeta potential value of the stem extract-mediated Co_3O_4 NPs suggests a higher tendency for particle agglomeration, leading to comparatively lower stability.

4. Conclusion

In summary, the Co_3O_4 nanoparticles were successfully synthesized in the combustion method using a green and cost-effective method involving the leaf, stem, and root of *Eichhornia crassipes* plant extract and urea as a fuel. The phytochemicals present in the plant extract acted as natural capping and stabilizing agents, promoting the formation of Co_3O_4 nanoparticles under controlled conditions. The X-ray diffraction studies confirm the formation of cobalt oxide nanoparticles with a cubic crystal structure. The bond lengths of Cobalt - Oxygen complexes are influencing the structural parameters. The transformation of anisotropic to isotropic behaviour can be expected due to substitution of Co^{3+} for Co^{2+} ions. Among them, the leaf-assisted sample showed the smallest crystallite size of 12.5 nm. The FT-IR analysis confirmed that the metal-oxygen vibrations below 1000 cm^{-1}, with occurrence of peaks at 650 cm^{-1} and 537 cm^{-1}, validated the successful synthesis of Co_3O_4 NPs with both tetrahedral and octahedral Co–O bonding. Co_3O_4 nanoparticles were analyzed using UV-visible diffuse reflectance spectroscopy (DRS), exhibited the direct band gap energies to be 3.29 eV, 3.37 eV, and 3.28 eV. A correlation was observed between particle size and band gap energy, where larger particles (18.90 nm) exhibited a lower band gap (3.28 eV). PL analysis confirmed the energy band gap and optical properties of Co_3O_4 NPs. FE-SEM analysis revealed a spherical morphology with agglomeration for leaf- and stem-assisted Co_3O_4 NPs, whereas root-assisted NPs exhibited porous, scattered spherical structures. EDX analysis confirmed the formation of Co_3O_4 nanoparticles by the occurrence of prominent peaks corresponding to cobalt (Co) and oxygen (O). The zeta potential values of cobalt oxide nanoparticles gave negative zeta potential values -41.9 mV (leaf) and -40.1 mV (root), which confirmed good particle colloidal stability. Furthermore, future work will focus on investigating the photocatalytic degradation efficiency of the synthesized Co_3O_4 nanoparticles. The *Eichhornia crassipes* itself possesses inherent photocatalytic properties due to its phytochemical constituents, and its synergistic role in assisting Co_3O_4 nanoparticle synthesis may enhance the overall photocatalytic performance for environmental remediation.

References

[1] S. Kumar, A. Kaur, J. Gaur, P. Singh, H. Kaur, S. Kaushal, J. Dalal, M. Misra State-of-the-art in Co_3O_4 nanoparticle synthesis and applications: Toward a sustainable future. Chemistry Select, 10(6), (2025) e202405147. https://doi.org/10.1002/slct.202405147

[2] S. Farhadi, J. Safabakhsh, P. Zaringhadam, Synthesis, characterization, and investigation of optical and magnetic properties of cobalt oxide (Co_3O_4) nanoparticles. Journal of Nanostructure in Chemistry, 3(1), (2013) 69. https://doi.org/10.1186/2193-8865-3-69

[3] B. Medina, M.G.V. Fressati, J. Martins Gonçalves, F. Maesta Bezerra, F.A. Pereira Scacchetti, M.P. Moisés, A. Bail, & R. Block Samulewski, Solventless preparation of Fe_3O_4 and Co3O4 nanoparticles: A mechanochemical approach. Materials Chemistry and Physics, 226, (2019) 318–322. https://doi.org/10.1016/j.matchemphys.2019.01.043

[4] A.M. Abdallah R. Awad, Sm and Er partial alternatives of Co in Co_3O_4 nanoparticles: Probing the physical properties. Physica B: Condensed Matter, 608, (2021) 412898. https://doi.org/10.1016/j.physb.2021.412898

[5] L. He, C. Chen, N. Wang, W. Zhou, L. Guo, Finite size effect on Néel temperature with Co_3O_4 nanoparticles. Journal of Applied Physics, 102(10), (2007) 103911. https://doi.org/10.1063/1.2817481

[6] A.K.M.A. Ullah, F.B. Amin, A. Hossain, Tailoring surface morphology and magnetic property by precipitants concentrations dependent synthesis of Co_3O_4 nanoparticles. Ceramics International, 46(18), (2020) 27892–27896. https://doi.org/10.1016/j.ceramint.2020.07.167

[7] M.H. Ahmad, R.B. Alam, A. Ul-Hamid, S.F.U. Farhad, M.R. Islam, Hydrothermal synthesis of Co_3O_4 nanoparticles decorated three dimensional MoS2 nanoflower for exceptionally stable supercapacitor electrode with improved capacitive performance. Journal of Energy Storage, 47, (2022) 103551. https://doi.org/10.1016/j.est.2021.103551

[8] M. Ghiasi, A. Malekzadeh, H. Mardani Synthesis and optical properties of cubic Co_3O_4 nanoparticles via thermal treatment of a trinuclear cobalt complex. Materials Science in Semiconductor Processing, 42, (2016) 311–318. https://doi.org/10.1016/j.mssp.2015.10.019

[9] S. Shah, H. Shaikh, S. Farrukh, M.I. Malik, Z.U.N. Mughal, S. Bhagat, Sonochemical synthesis of Co_3O_4 nanoparticles deposited on GO sheets and their potential application as a nanofiller in MMMs for O2/N2 separation. RSC Advances, 11, (2021) 19647.

https://doi.org/10.1039/D1RA02264D

[10] Y. Chen, S. Wang, Z. Chen, Y. Ding, L. Zhang, L. Lv, Y. Wang, D. Xu, S. Wang, Synthesis of Co_3O_4 nanoparticles with controllable size and their catalytic property. Solid State Sciences, 82, (2018) 78–83. https://doi.org/10.1016/j.solidstatesciences.2018.06.004

[11] C.I. Priyadharsini, G. Marimuthu, T. Pazhanivel, P.M. Anbarasan, V. Aroulmoji, V. Siva, L. Mohana, Sol–Gel synthesis of Co_3O_4 nanoparticles as an electrode material for supercapacitor applications. Journal of Sol-Gel Science and Technology, 96, (2020) 416–422 https://doi.org/10.1007/s10971-020-05393-x

[12] S.Z. Mohammadi, B. Lashkari, A. Khosravan, Green synthesis of Co_3O_4 nanoparticles by using walnut green skin extract as a reducing agent by using response surface methodology. Surfaces and Interfaces, 23, (2021) 100970. https://doi.org/10.1016/j.surfin.2021.100970

[13] N.R. Khalid, A. Gull, F. Ali, M.B. Tahir, T. Iqbal, M. Rafique, M.A. Assiri, M. Imran, M. Alzaid Bi-functional green-synthesis of Co3O4 NPs for photocatalytic and electrochemical applications. Ceramics International, 48(21), (2022) 32009–32021. https://doi.org/10.1016/j.ceramint.2022.07.138

[14] A. Diallo, A.C. Beye, T.B. Doyle, E. Park, M. Maaza, Green synthesis of Co_3O_4 nanoparticles via Aspalathus linearis: Physical properties. Green Chemistry Letters and Reviews, 8(1), (2015) 30–36. https://doi.org/10.1080/17518253.2015.1082646

[15] N.O.M. Dewi, Y. Yulizar, D.O.B. Apriandanu, Green synthesis of Co_3O_4 nanoparticles using Euphorbia heterophylla, L. leaves extract: Characterization and photocatalytic activity. IOP Conference Series: Materials Science and Engineering, 509, (2019) 012105. https://doi.org/10.1088/1757-899X/509/1/012105

[16] C.A. Paul, E.R. Kumar, A.F. Abd El-Rehim, G. Yang, Cobalt oxide nanoparticles for biological applications: Synthesis and physicochemical characteristics for different natural fuels. Ceramics International, 49(24), (2023) 40244–40257. https://doi.org/10.1016/j.ceramint.2023.09.360

[17] B.K. Palai, S.K. Sarangi, S.S. Mohapatra, Investigation of physiochemical and thermal properties of Eichhornia crassipes fibers. Journal of Natural Fibers, 18, (2019) 1320–1331. https://doi.org/10.1080/15440478.2019.1691110

[18] S. Gopinath, K. Sivakumar, B. Karthikeyen, C. Ragupathi, R. Sundaram Structural, morphological, optical and magnetic properties of Co_3O_4 nanoparticles prepared by conventional method. Physica E: Low-dimensional Systems and Nanostructures, 81, (2016) 66–70. https://doi.org/10.1016/j.physe.2016.02.006

[19] P. Chelliah, S. M. Wabaidur, H.P. Sharma, M.J. Jweeg, H.S. Majdi, M.M.R.AL. Kubaisy, A. Iqbal, W.C. Lai, Green synthesis and characterizations of cobalt oxide nanoparticles and their coherent photocatalytic and antibacterial investigations. Water, 15, (2023) 910. https://doi.org/10.3390/w15050910

[20] R. Anupriya, V. Kalaiselvi, P. Yasotha, S. Gopi, Sustainable Green Synthesis of ZnO Nanoparticles using Syzygium Cumini Fruit Extract: Structural, Optical, and Antibacterial Investigations, NanoNEXT, 6(4), 1–9. https://doi.org/10.54392/nnxt2541

[21] M. Alzaid, A.M. Abu-Dief, N.M.A. Hadia, M. Ezzeldien, W.S. Mohamed, Synthesis and characterization study of spinel Co3O4 nanoparticles synthesized via the facial co-precipitation route for optoelectronic application. Optical and Quantum Electronics, 56, (2024)1156. https://doi.org/10.1007/s11082-024-07095-y

[22] D. Su, S. Dou, G. Wang. Single crystalline Co3O4 nanocrystals exposed with different crystal planes for Li-O_2 batteries. Scientific Reports, 4, (2014) 5767. https://doi.org/10.1038/srep05767

[23] A.A.P. Selva Filho, F.C.G. Almeida, R.C.F. Soares da Silva, L.A. Sarubbo, Analysis of the surfactant properties of Eichhornia crassipes for application in the remediation of environments impacted by hydrophobic pollutants. Biocatalysis and Agricultural Biotechnology, 36, (2021) 102120. https://doi.org/10.1016/j.bcab.2021.102120

[24] D.D. M. Prabaharan, K. Sadaiyandi, M. Mahendran, S. Sagadevan Precipitation method and characterization of cobalt oxide nanoparticles. Applied Physics A, 123(264), (2017). https://doi.org/10.1007/s00339-017-0786-8

[25] M. Hafeez, R. Shaheen, B. Akram, Zain-ul-Abdin, S. Haq, S. Mahsud, S. Ali, R.T. Khan, Green synthesis of cobalt oxide nanoparticles for potential biological applications. Materials Research Express, 7, (2020) 025019. https://doi.org/10.1088/2053-1591/ab70dd

[26] H. Alhussain, A.M. Alghamdi, N.Y. Elamin, A. Rajeh, Recent progress in enhanced optical, mechanical, thermal properties and antibacterial activity of the chitosan/polyvinylalcohol/Co_3O_4 nanocomposites for optoelectronics and biological applications. Journal of Polymers and the Environment, 32, (2024) 3735–3748. https://doi.org/10.1007/s10924-024-03191-y

[27] M.B. Muradov, S.J. Mammadyarova, G.M. Eyvazova, O.O. Balayeva, S.Z. Melikova, N. Sadigov, M.I. Abdullayev, N. Musayeva, E.K. Gasimov, F.H. Rzayev, I. Hasanova,

Sonochemical synthesis and characterization of structural, optical and dielectric properties of Ag-doped Co_3O_4 nanoparticles. Journal of Cluster Science, 35, (2024) 845–861. https://doi.org/10.1007/s10876-023-02514-8

[28] Shriya Tripathi, Narendra Kumar Pandey, Vernica Verma, Comparative Investigation of Structural, Optical and Morphological properties of Manganese Oxide and its composite, NanoNEXT, 5(4), 11–15. https://doi.org/10.54392/nnxt2442

[29] T. Lohitha, H.M. Albert, Investigating the structural, spectroscopic, photoluminescence, and antibacterial characteristics of biosynthesized cobalt-infused cerium oxide nanoparticles. Journal of Materials Research, 40, (2025) 1279–1291. https://doi.org/10.1557/s43578-025-01579-7

Authors Contribution Statement

K. Leninbarathi: Conceptualization, Methodology, Investigation, Formal analysis, Validation, Writing Original Manuscript. G. Bharath: Investigation. S. Sathiyaraj: Formal Analysis. E. Ranjith Kumar: Validation. Ch. Srinivas: Formal Analysis. Vinayakprasanna N. Hegde: Writing Review and Editing, R.T. Karunakaran: Conceptualization, Supervision, Writing, Review and Editing. All the Authors read and approved the final version of the manuscript.

Funding

The authors declare that no funds, grants or any other support were received during the preparation of this manuscript.

Competing Interests

The authors declare that there are no conflicts of interest regarding the publication of this manuscript.

Data Availability

The data supporting the findings of this study can be obtained from the corresponding author upon reasonable request.

Has this article screened for similarity?

Yes

About the License